STELLAR ENCOUNTERS WITH THE β PICTORIS PLANETESIMAL SYSTEM

PAUL KALAS[1] AND JEAN-MARC DELTORN[2]

Space Telescope Science Institute, 3700 San Martin Drive, Baltimore, MD 21218

AND

JOHN LARWOOD

Astronomy Unit, Queen Mary and Westfield College, London, E1 4NS, UK

Received 2000 May 8; accepted 2001 January 24

ABSTRACT

We use data from the *Hipparcos* catalog and the Barbier-Brossat & Figon catalog of stellar radial velocities to test the hypothesis that the β Pic planetesimal disk was disrupted by a close stellar encounter. We trace the space motions of 21,497 stars and discover 18 that have passed within 5 pc of β Pic in the past 1 Myr. β Pic's closest encounter is with the K2 III star HIP 27628 ($\sim$0.6 pc), but dynamically the most important encounter is with the F7 V star HIP 23693 ($\sim$0.9 pc). We calculate the velocity and eccentricity changes induced by the 18 perturbations and conclude that they are dynamically significant if planetesimals exist in a β Pic Oort cloud. We provide a first-order estimate for the evolutionary state of a β Pic Oort cloud and conclude that the primary role of these stellar perturbations would be to help build a comet cloud rather than destroy a preexisting structure. The stellar sample is $\sim$20% complete and motivates future work to identify less common close interactions that would significantly modify the observed circumstellar disk. For future radial velocity study, we identify six stars in the *Hipparcos* catalog that may have approached β Pic to within 0.1 pc and therefore remain as candidate disk perturbers.

Subject headings: circumstellar matter — planetary systems — stars: individual (β Pictoris)

On-line material: color figure

1. INTRODUCTION

The dynamical mechanisms that dominate the formation and subsequent evolution of planetary systems can be broadly described as either endogenic or exogenic in origin. The formation of giant planets and their apparent orbital migration (Goldreich & Tremaine 1980; Malhotra, Duncan, & Levison 2000; Marcy, Cochran, & Mayor 2000b) is probably the most significant endogenic source for modifying a planetary system over time. In our solar system, the giant planets have displaced a significant fraction of small bodies from their formation sites to either the Oort cloud or interstellar space. For circumstellar dust disks observed around nearby main-sequence stars, unseen giant planets are believed to produce the ubiquitous central depletions in the dust distributions (Roques et al. 1994; Pantin, Lagage, & Artymowicz 1997; Greaves et al. 1998; Liou & Zook 1999; Wyatt et al. 1999).

However, young systems, such as pre–main-sequence stars in clusters and the proplyd objects in Orion, experience significant exogenic forces (Larwood 1997). Close stellar encounters with other cluster members (Laughlin & Adams 1998) and radiation pressure from nearby massive stars (Henney & O'Dell 1999) remove disk material and can disrupt the vertical settling of circumstellar dust and gas. During the evolution of our solar system, the Galactic tide and encounters with molecular clouds and passing stars decoupled comets from the planetary region, preserving them in the Oort cloud (Oort 1950; Fernandez 1997).

The dust disk around the A5 V star β Pic displays evidence for both types of dynamical mechanism. A planet may be responsible for clearing dust within a $\sim$20 AU radius of the star (Smith & Terrile 1984; Lagage & Pantin 1994), perturbing families of comets toward the stellar photosphere (Beust & Morbidelli 2000), vertically disrupting the disk at 50 AU radius (Burrows et al. 1995; Mouillet et al. 1997; Heap et al. 2000), and creating a few hour duration, 0.06 mag, achromatic drop in β Pic's light curve (Lecavelier des Etangs et al. 1997). A recent and close stellar flyby perturbation may be responsible for producing the radially and vertically asymmetric disk structure at large radii (Kalas & Jewitt 1995), as well as substructure in one disk midplane between 500 and 800 AU projected radius (Kalas et al. 2000; Larwood & Kalas 2001). Since the age of β Pic is between 8 Myr (Crifo et al. 1997) and 20 Myr (Barrado y Navascues et al. 1999), understanding the dynamics of objects surrounding β Pic could elucidate conditions and events that determined the early evolution of our solar system.

Here we examine possible exogenic perturbations on β Pic. A key piece of observational evidence needed to confirm the stellar flyby hypothesis is to identify a perturbing star. Given improved trigonometric parallaxes and proper motions from *Hipparcos* (European Space Agency 1997), we are motivated to test the stellar flyby hypothesis empirically. Section 2 presents our method for using *Hipparcos* and radial velocity data to trace the Galactocentric motions of stars relative to β Pic. Section 3 identifies stars that have passed within 5 pc of β during the past 1 Myr. In § 4 we assess the significance of the stellar encounters for the evolution of a possible Oort cloud around β Pic. Section 5 demonstrates the plausibility of very close stellar encoun-

[1] Current Address: Department of Astronomy, 601 Campbell Hall, University of California, Berkeley, CA 94720; kalas@stsci.edu.

[2] Laboratoire d'Astrophysique de Marseille, Traverse du Siphon, Les trois-Lucs, 13376, Marseille Cedex 12, France.

TABLE 1

Input Parameters for the Stars with $D_{ca} < 5$ pc

Hipparcos	HD	Other	π (mas)	σ_π (mas)	α_{1950}	δ_{1950}	l_{1950} (deg)	b_{1950} (deg)	R_V (km s^{-1})	σ_{R_V} (km s^{-1})	$pm(\alpha)$ (mas)	$\sigma_{pm(\alpha)}$ (mas)	$pm(\delta)$ (mas)	$\sigma_{pm(\delta)}$ (mas)	Spectral Type	Notes
27321......	39060	β Pic	51.87	0.51	05 46 05.93	-51 05 01.8	258.36	-30.61	19.83	0.67	4.65	0.53	81.96	0.61	A5 V	
10798......	14412	HR 683	78.88	0.72	02 16 44.06	-26 10 53.2	214.45	-70.41	7.00	0.50	-218.07	0.60	444.51	0.48	G5 V	High proper motion star
17378......	23249	δ Eri	110.58	0.88	03 40 51.03	-09 55 52.9	198.09	-46.00	-6.00	0.70	-91.71	0.98	742.23	0.92	K0 IV	Variable of RS CVn type
19893......	27290	γ Dor	49.26	0.50	04 14 42.85	-51 36 43.2	259.83	-44.78	25.20	1.20	100.57	0.46	184.23	0.50	F4 III	Pulsating variable Star
19921......	27442	ϵ Ret	54.84	0.50	04 15 37.02	-59 25 18.7	270.20	-42.56	29.30	0.50	-47.99	0.52	-167.81	0.50	K2 IVa	Star in double system
22122......	30501	G J176.3	48.90	0.64	04 44 22.88	-50 09 32.5	256.99	-40.37	17.00	2.50	-445.81	0.59	-337.31	0.66	K 1V	High proper motion star
23693......	33262	ζ Dor	85.83	0.46	05 04 39.05	-57 32 25.6	266.03	-36.72	-2.10	0.40	-31.87	0.46	117.42	0.48	F7 V	
25544......	36435	G J204.1	51.10	0.52	05 27 03.23	-60 27 15.3	269.31	-33.62	12.90	1.20	-148.89	0.56	-92.83	0.64	G6/G8 V	High proper motion star
27628......	39425	β Col	37.94	0.57	05 49 11.74	-35 47 09.6	241.34	-27.06	89.10	0.80	55.74	0.50	404.68	0.47	K2 III	High proper motion star
29568......	43162	HR 2225	59.90	0.75	06 11 41.23	-23 50 53.0	230.85	-18.52	22.30	0.30	-47.06	0.45	110.90	0.62	G5 V	
29958......	...	G J9210	32.30	2.10	06 16 04.60	-13 51 09.6	221.79	-13.51	103.80	2.00	66.60	1.91	341.18	1.64	M0 IV	Double or multiple star
31711......	48189	HR 2468	46.15	0.64	06 37 28.46	-61 29 19.5	271.20	-25.20	32.30	0.30	-50.08	0.73	72.69	0.66	G1.5 V	Star in double system
37504......	63295	ζ Vol	24.36	0.48	07 42 26.97	-72 29 10.6	284.57	-22.16	48.10	0.50	33.38	0.44	15.29	0.40	K0 III	
38908......	65907	G J294A	61.76	0.51	07 56 51.58	-60 10 06.1	273.38	-15.68	14.10	1.20	518.38	0.63	118.86	0.51	G0 V	High proper motion star
83990......	154577	G J656	73.07	0.91	17 05 40.03	-60 40 27.1	329.82	-12.22	8.80	1.20	71.14	0.76	589.82	0.62	K2 V	High proper motion star
89042......	165499	ι Pav	56.32	0.68	18 05 47.26	-62 00 55.1	332.21	-19.16	29.70	1.20	-77.60	0.59	234.68	0.44	G0 V	High proper motion star
93506......	176687	ζ Sag	36.61	1.37	18 59 25.89	-29 57 12.3	6.84	-15.35	24.10	3.30	-14.10	2.62	3.66	2.00	A2 III	Double or multiple star
114996......	219571	γ Tuc	45.40	0.61	23 14 31.51	-58 30 36.7	324.30	-54.82	18.40	0.50	-34.93	0.44	79.59	0.50	F1 III	
116250......	221420	G J4340	31.49	0.49	23 30 08.40	-77 39 42.2	308.32	-38.91	26.00	1.20	15.66	0.51	1.79	0.43	G2 V	

Note.—Units of right ascension are hours, minutes, and seconds, and units of declination are degrees, arcminutes, and arcseconds.

ters and presents a list of candidate perturbers for future radial velocity observations.

2. SEARCH FOR β PIC STELLAR PERTURBERS

We search for candidate β Pic perturbers using data from the entire *Hipparcos* catalog and the Barbier-Brossat & Figon (2000) catalog of stellar radial velocities. The *Hipparcos* catalog gives the positions, proper motions, and parallaxes of 118,218 stars from which we compute the Galactocentric coordinates. Barbier-Brossat & Figon (2000) provide the mean radial velocities for 36,145 stars, of which 21,497 stars are also contained in the *Hipparcos* catalog. We combine the radial velocities with the *Hipparcos* proper motion data (Johnson & Soderblom 1987) to trace the space trajectories of the 21,497 stars during the past 1 Myr.

The observed disk substructure should be short-lived, because of orbital phase mixing. The dynamical models of Kalas et al. (2000) and Larwood & Kalas (2001) indicate that the perturbation occurred as recently as 10^5 yr ago. However, we choose to extend the search 1 Myr into the past to allow for the uncertainties introduced by the assumptions inherent in the models.

Key factors limiting the completeness of the search are the sensitivity constraints imposed by the two catalogs. In general, we expect that a significant fraction of late-type stars near β Pic ($d = 19.3$ pc) is undetected. For spectral types later than G5, volume 1 of the *Hipparcos* catalog states a completeness limit: $m_v \leq 7.3 + 1.1 \, |\sin(b)|$, where b is the Galactic latitude. For β Pic, $b \sim -30°$, giving a completeness limit of $m_v \leq 7.85$ mag. At $d = 20$ pc this translates to $M_v \leq 6.3$ mag, which corresponds to the absolute magnitude of a K2 V star (Cox 1999). At $d = 30$ pc, $M_v \leq 5.5$ mag, which is the absolute magnitude of a K0 V star (Cox 1999). Thus, the *Hipparcos* catalog includes a significant fraction of the A–G spectral types in a 10 pc radius volume around β Pic, but will miss K and M dwarfs (in Kalas et al. 2000, the β Pic disk perturber has a mass consistent with an M dwarf).

Estimating the completeness of the Barbier-Brossat & Figon (2000) catalog is considerably more difficult because it is not an all-sky survey, and the radial velocity information derives from different sources. Even though the majority of stars are $m_v \leq 10$ mag, comparable to the sensitivity limit of the *Hipparcos* catalog, the *Hipparcos* catalog contains more than 3 times as many stars. The incompleteness of our sample therefore exceeds 50%, and in § 3 we estimate an incompleteness of $\sim 80\%$. Future missions such as *FAME*, *SIM*, and *GAIA* will have the sensitivity to significantly improve the perturber search if radial velocity catalogs are also expanded.

For β Pic's radial velocity, we choose the recent measurement given by Grenier et al. (1999) because the published error, σ_{RV}, is smaller than that determined by Barbier-Brossat & Figon (2000). Experimental trials using other published radial velocities for β Pic (e.g., Lagrange et al. 1995) show negligible differences from the results presented below.

The relatively short timescale considered here permits a first-order estimate of the stellar trajectories using a straight-line motion approximation. A correction for the two-body interaction is only significant for very close ($\lesssim 10^{-2}$ pc) and low relative velocity ($\lesssim 10$ km s^{-1}) encounters. For each of the 21,497 stars we calculate a trajectory backward in time and determine the closest approach distance, D_{ca} (pc), to β Pic and the time of closest approach, t_{ca} (kyr), where $t_{ca} = 0$ is the present. To test the validity of the linear approximation for deriving trajectories, we use a fourth-order Runge-Kutta scheme to solve the equation of motion in the Galactic potential for six of the 18 stars that approach within 5 pc of β Pic. We adopt the axisymmetric Milky Way mass distribution model provided by Allen & Santillán (1991). This model[3] has proved to be well adapted to the calculations of orbits (de Boer et al. 1997) and has already been applied to the motions of globular clusters and nearby stars (Allen & Santillán 1993; Schuster & Allen 1997). In the Galactocentric cylindrical coordinates (R, θ, z), the small value of z/R in the range of time considered here permits the decoupling of motions in the Galactic plane and on the z-axis. We check our calculations by reproducing the published results on the nearest approaches of stars with the Sun (García-Sánchez et al. 1999; Müllari & Orlov 1996; Matthews 1994). The initial coordinates and velocities have been changed from the heliocentric to the Galactocentric reference frame using the current IAU values for the LSR ($\dot{\theta}_{LSR} = 220$ km s^{-1}, $R_{LSR} = 8.5$ kpc). As expected, the agreement between the D_{ca} and t_{ca} values derived from the straight-line approximation and the ones calculated from the integrated Galactic orbits allows us to restrict our computations to the linear case for the selection of candidates.

The main advantage of adopting the linear approximation is that we can determine the influence of the errors for the input positions and velocities on the estimate of D_{ca} and t_{ca} through a Monte Carlo draw. We use the standard deviations provided in the *Hipparcos* catalog and the Barbier-Brossat & Figon (2000) catalog. We assume a Gaussian distributions for the errors, centered on the average value and with dispersion equal to σ_{rms}. We produce 10^4 random draws that for each star lead to a probability distribution in the closest approach plane (D_{ca}, t_{ca}).

Table 1 lists the stars that approached within 5 pc of β Pic during the past 1 Myr. For this subset of stars we then use SIMBAD to search the literature for recent radial velocity measurements that may not have been included in the Barbier-Brossat & Figon (2000) catalog. Grenier et al. (1999) have measured the radial velocity for HIP 19893 and give a smaller measurement error than that listed by Barbier-Brossat & Figon (2000). We therefore recalculate the space trajectory and errors using the Grenier et al. (1999) radial velocity, which is given in Table 1. We make the same correction for HIP 17378, which has a more accurate radial velocity measurement from De Medeiros & Mayor (1999). As with β Pic, trials using different published radial velocity measurements for each star produce negligible changes in the final values of D_{ca} and t_{ca}.

3. CANDIDATE PERTURBERS WITH $D_{ca} < 5$ pc

From the 21,497 stars selected from the *Hipparcos* catalog and the Barbier-Brossat & Figon (2000) catalog, 18 are found to have $D_{ca} < 5$ pc with respect to β Pic in $-10^6 < t_{ca} < 0$ yr. Table 1 lists the values of their respective trajectory parameters. Columns (2) and (3) in Table 2 give the maxima and 1 σ uncertainties for the probability density distributions derived from the Monte Carlo draws

---

[3] Consisting of a spherical central bulge, a Miyamoto & Nagai (1975) disk, and a massive spherical halo.

TABLE 2

CHARACTERISTICS OF THE CLOSEST APPROACH FOR THE STARS WITH $D_{ca} < 5$ pc

No. (1)	Hipparcos Name (2)	t_{ca} (kyr) (3)	D_{ca} (pc) (4)	$P_{95.4\%}(<1$ pc$)$ $(P_{68.3\%}(<1$ pc$))$ (%) (5)	$P_{95.4\%}(<0.5$ pc$)$ $(P_{68.3\%}(<0.5$ pc$))$ (%) (6)
1.......	HIP 10798	$-318.2^{+11.7}_{-14.6}$	$1.88^{+0.51}_{-0.40}$	2.49 (0.00)	0.00 (0.00)
2.......	HIP 17378	$-294.7^{+16.6}_{-17.9}$	$3.96^{+0.42}_{-0.41}$	0.00 (0.00)	0.00 (0.00)
3.......	HIP 19893	$-31.1^{+35.2}_{-36.3}$	$4.94^{+0.19}_{-0.14}$	0.00 (0.00)	0.00 (0.00)
4.......	HIP 19921	$-118.9^{+11.7}_{-8.9}$	$3.74^{+0.31}_{-0.33}$	0.00 (0.00)	0.00 (0.00)
5.......	HIP 22122	$-34.0^{+5.9}_{-5.8}$	$2.76^{+0.56}_{-0.18}$	0.00 (0.00)	0.00 (0.00)
6.......	HIP 23693	$-356.3^{+29.3}_{-32.2}$	$0.92^{+0.13}_{-0.12}$	54.16 (53.42)	0.00 (0.00)
7.......	HIP 25544	$-116.0^{+8.8}_{-9.1}$	$1.49^{+0.39}_{-0.30}$	0.00 (0.00)	0.00 (0.00)
8.......	HIP 27628	$-107.2^{+14.6}_{-11.7}$	$0.58^{+0.51}_{-0.11}$	70.28 (71.85)	3.10 (2.75)
9.......	HIP 29568	$-693.2^{+43.9}_{-46.9}$	$2.95^{+0.90}_{-0.32}$	0.00 (0.00)	0.00 (0.00)
10......	HIP 29958	$-198.0^{+32.2}_{-29.3}$	$1.00^{+2.36}_{-0.40}$	10.21 (12.76)	0.70 (0.00)
11......	HIP 31711	$-189.3^{+49.8}_{-76.2}$	$3.97^{+0.37}_{-0.31}$	0.00 (0.00)	0.00 (0.00)
12......	HIP 37504	$-643.4^{+52.7}_{-38.1}$	$4.59^{+1.52}_{-0.91}$	0.00 (0.00)	0.00 (0.00)
13......	HIP 38908	$-139.7^{+5.9}_{-8.7}$	$1.97^{+0.69}_{-0.42}$	0.00 (0.00)	0.00 (0.00)
14......	HIP 83990	$-303.5^{+17.6}_{-14.6}$	$3.92^{+1.18}_{-1.16}$	0.00 (0.00)	0.00 (0.00)
15......	HIP 89042	$-397.3^{+20.5}_{-23.4}$	$2.29^{+1.21}_{-0.21}$	0.00 (0.00)	0.00 (0.00)
16......	HIP 93506	$-910.0^{+137.7}_{-128.1}$	$3.50^{+2.31}_{-1.21}$	0.00 (0.00)	0.00 (0.00)
17......	HIP 114996	$-596.5^{+32.6}_{-42.7}$	$3.94^{+1.35}_{-1.77}$	0.00 (0.00)	0.00 (0.00)
18......	HIP 116250	$-883.6^{+61.5}_{-67.4}$	$2.79^{+2.39}_{-1.92}$	3.66 (2.74)	0.08 (0.00)

for (D_{ca}, t_{ca}). Figure 1 shows the D_{ca} and t_{ca} values resulting from the Monte Carlo draw for a subset of stars with $D_{ca} < 3$ pc. Figure 2 presents the results in the form of isocontours representing the 68.3%, 95.4%, and 99.5% confidence levels for finding a star within a given region in the close-encounter plane (D_{ca}, t_{ca}). An encounter probability is determined by dividing the contour area below a specified closest approach limit by the total contour area in the D_{ca}, t_{ca} plane. The probabilities that each star approached <1 pc and <0.5 pc with confidence levels of 95.4% and 68.3% are listed in columns (5) and (6) of Table 2.

Three stars (HIP 23693, HIP 27628, and HIP 29958) have $D_{ca} < 1$ pc. However, the greater uncertainties in the observables for HIP 29958 (Table 1) mean that there is only a 10% probability at the 95.4% confidence level that its closest approach was <1 pc. For HIP 23693 and HIP 27628, the probabilities that $D_{ca} < 1$ pc are greater than 50%. HIP 93506 and HIP 116250 are notable because $2–3 \times 10^5$ yr before their closest approach to β Pic (Table 2), they passed <3 pc from the Sun (García-Sánchez et al. 1999).

The incompleteness of our sample is evident by comparing the number of candidate perturbers found by this experiment to the number expected. If we assume that β Pic's heliocentric distance, $d = 19.3$ pc, places it within the solar neighborhood, then the stellar encounter frequency should be roughly equal to that of the Sun: $N = 12.4$ Myr^{-1} for $D_{ca} \leq 1$ pc (García-Sánchez et al. 1999). Thus, our search produces a factor of ~ 5 too few perturbers. Using the *Hipparcos* catalog, García-Sánchez et al. (1999) give their empirical finding that $N \geq 3.5D_{ca}^{2.12}$ Myr^{-1}, and they conclude that their sample is incomplete by at least 50%. For our $D_{ca} < 5$ pc cutoff, the empirical relation given by García-Sánchez et al. (1999) yields $N \geq 106$ Myr^{-1}, but for β Pic we find $N = 18$ Myr^{-1} (Table 1). Again, the discrepancy indicates that our sample is $\sim 20\%$ complete. Thus, we expect that a volume-limited search realized with future stellar catalogs will reveal at least $\sim 10^2$ stars approaching β Pic within 5 pc.

To determine which candidate perturber had the greatest dynamical impact on β Pic, we factor in the relative stellar masses and velocities. We calculate the velocity impulse Δv due to each stellar passage on both a β Pic disk particle ($r = 10^3$ AU) and on a hypothetical Oort cloud object ($r = 10^5$ AU). Under the impulse approximation, the change of velocity Δv of a comet relative to β Pic due to the
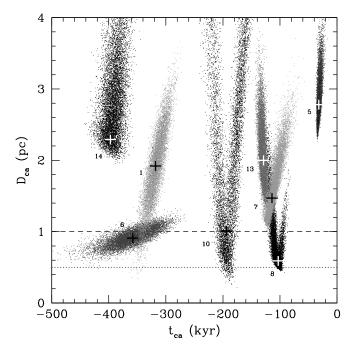

FIG. 1.—Positions in the closest approach plane (D_{ca}, t_{ca}) from the random Monte Carlo draw. From the 18 candidate perturbers, we show a subsample of eight stars that have $D_{ca} < 3$ pc. Each color corresponds to a different star, which have number labels corresponding to column (1) in Tables 2 and 3. Crosses mark the maxima of the probability distributions for (D_{ca}, t_{ca}). The spread in the distribution of points reflects the initial uncertainties on the stellar proper motions, parallaxes, and radial velocities. The horizontal dashed line marks $D = 1.0$ pc ($\simeq$ β Pic's Roche radius), and the dotted line marks $D = 0.5$ pc. [*See the electronic edition of the Journal for a color version of this figure.*]
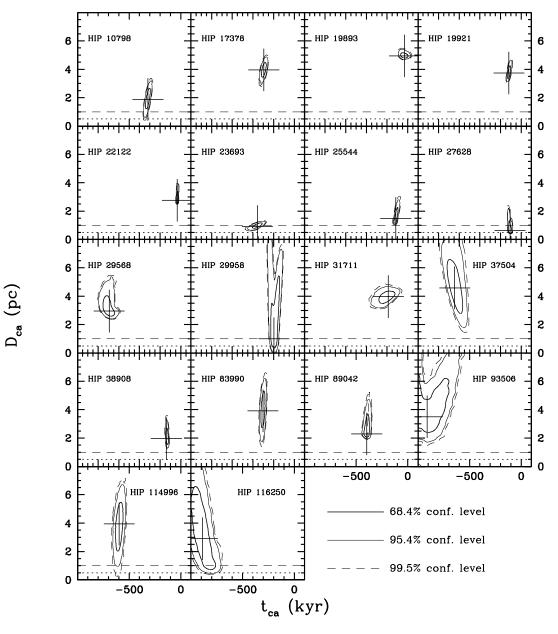
Fig. 2.—Isocontours for the Monte Carlo distributions in the closest approach plane (D_{ca}, t_{ca}) for the 18 stars with $D_{ca} < 5$ pc. *Bold contour*: 68.3% confidence level; *thin contour*: 95.4%; *dashed contour*: 99.5% confidence level. The contours outline the decreasing probability of finding the star at a more specific location at a given time because of uncertainties in proper motion, radial velocity, and parallax. Each cross marks the position of the maximum of the probability density distribution in the Monte Carlo simulation (the size of the crosses has no significance). The probabilities that are given in columns (5) and (6) of Table 2 are calculated by dividing the area for each contour below the 1 pc and 0.5 pc lines by the total area enclosed by the contour. Second figure shows enlarged plot for the four candidate perturbers with the smallest D_{ca}.

influence of a passing star can be approximated as

$$\Delta v^2 = \left(\frac{2\mathscr{G}M_*}{\Delta V_{ca} D_{ca}}\right)^2 \frac{r^2}{r^2 + D_{ca}^2 - 2rD_{ca}\cos\beta}, \quad (1)$$

where M_* is the mass of the passing star, ΔV_{ca} is the relative velocity, D_{ca} and r are the distances from β Pic to the passing star and to a comet, respectively, and β denotes the angle between r and D_{ca} at the time of closest approach (Oort 1950; Fernandez & Ip 1991).

From Δv we can also estimate the change in eccentricity, Δe, using the following result from numerical simulations (Brunini & Fernandez 1996): $\Delta e \sim 2\Delta v/v$, where the comet's orbital velocity v is $v^2 = \mathscr{G}M_{\beta\,Pic}/r$. Integrating equation (1)

over β, we compute the average perturbation of a given close encounter on a shell of comets at distance r. The resulting Δv and Δe for both the maximum perturbation ($\beta = 0$) and the average one at $r = 10^5$ AU are compiled in Table 3, together with the 1 σ uncertainties deduced from our Monte Carlo draws, and plotted in Figures 3 and 4. For $r = 10^3$ AU, the values for Δv and Δe are smaller by a factor determined from equation (1). For example, in the HIP 23693 encounter, Δv_{max} is a factor of 4.4×10^4 smaller, and Δe_{max} is 4.4×10^5 smaller.

Among the initial best candidates, HIP 27628 (No. 8) produces the greatest Δv_{max} on particles located between itself and β Pic ($\Delta v_{max} \simeq 0.7$ m s^{-1}) at the time of closest approach (Table 3). However, its effect on the whole cloud is

HIP 10798

HIP 23693
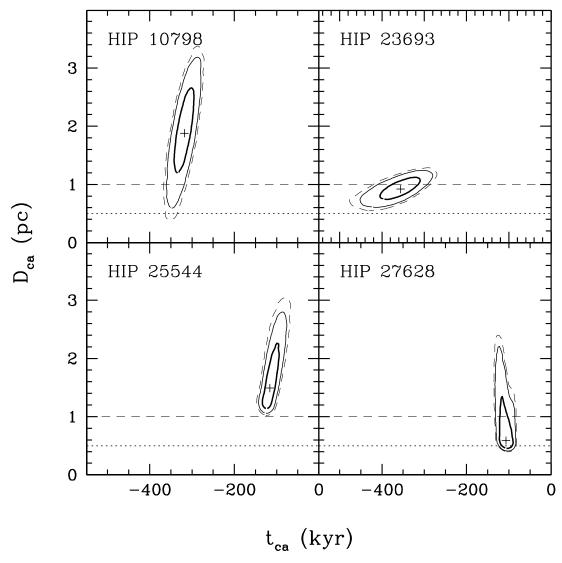
HIP 25544

HIP 27628

D_{ca} (pc)

t_{ca} (kyr)

Fig. 2.—*Continued*

TABLE 3

Dynamical Influence of the Close Encounters on Objects Orbiting β Pic at 10^5 AU

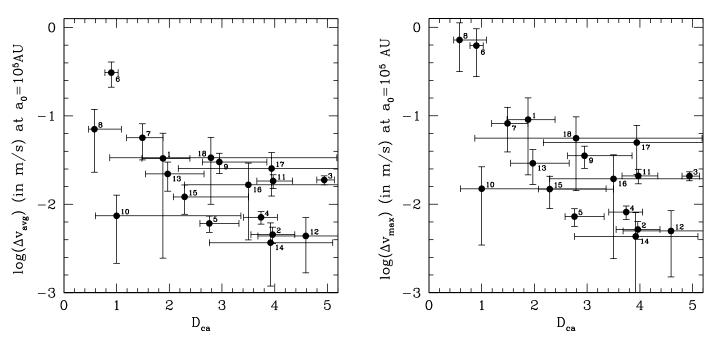| No.	*Hipparcos* Name	Spectral Type	Mass $(M_\odot)$	D_{ca} (pc)	ΔV_{ca} (km s^{-1})	Δv_{avg} (10^{-3} m s^{-1})	Δv_{max} (10^{-3} m s^{-1})	Δe_{avg} (10^{-3})	Δe_{max} (10^{-3})	R_{eq} (pc)
1	HIP 10798	G5 V	0.9	$1.88^{+0.51}_{-0.40}$	42.8 ± 1.3	33.07 ± 30.61	90.52 ± 69.02	0.54 ± 0.45	1.47 ± 0.92	$1.09^{+0.30}_{-0.23}$
2	HIP 17378	K0 IV	0.8	$3.96^{+0.42}_{-0.41}$	47.9 ± 1.5	4.55 ± 0.96	5.19 ± 1.17	0.07 ± 0.02	0.08 ± 0.02	$2.35^{+0.25}_{-0.24}$
3	HIP 19893	F4 III	1.5	$4.94^{+0.19}_{-0.14}$	13.4 ± 1.4	18.86 ± 2.19	20.85 ± 2.45	0.31 ± 0.04	0.34 ± 0.04	$2.55^{+0.10}_{-0.07}$
4	HIP 19921	K2 IVa	0.7	$3.74^{+0.31}_{-0.33}$	28.6 ± 0.6	7.13 ± 1.15	8.16 ± 1.41	0.12 ± 0.02	0.13 ± 0.02	$2.28^{+0.19}_{-0.20}$
5	HIP 22122	K1 V	0.8	$2.76^{+0.56}_{-0.42}$	62.7 ± 1.5	6.08 ± 1.27	7.26 ± 1.63	0.10 ± 0.02	0.12 ± 0.03	$1.64^{+0.33}_{-0.25}$
6	HIP 23693	F7 V	1.4	$0.92^{+0.13}_{-0.11}$	21.6 ± 1.5	308.70 ± 97.73	621.14 ± 344.07	5.03 ± 1.59	10.12 ± 5.60	$0.48^{+0.07}_{-0.06}$
7	HIP 25544	G6/G8 V	0.9	$1.49^{+0.39}_{-0.30}$	25.5 ± 0.9	56.59 ± 24.86	81.96 ± 42.86	0.92 ± 0.40	1.33 ± 0.70	$0.86^{+0.23}_{-0.17}$
8	HIP 27628	K2 III	0.7	$0.58^{+0.51}_{-0.11}$	83.9 ± 2.1	70.82 ± 47.74	719.08 ± 403.24	1.15 ± 0.78	11.71 ± 7.04	$0.35^{+0.31}_{-0.07}$
9	HIP 29568	G5 V	0.9	$2.95^{+0.90}_{-0.32}$	11.6 ± 0.5	30.09 ± 7.77	35.36 ± 9.88	0.49 ± 0.13	0.58 ± 0.16	$1.71^{+0.52}_{-0.19}$
10	HIP 29958	M0 IV	0.5	$1.00^{+2.36}_{-0.40}$	102.1 ± 5.6	7.42 ± 5.27	14.98 ± 11.52	0.12 ± 0.10	0.24 ± 0.17	$0.65^{+1.53}_{-0.26}$
11	HIP 31711	G1.5 V	1.0	$3.97^{+0.37}_{-0.31}$	14.6 ± 1.4	18.37 ± 3.26	20.93 ± 3.90	0.30 ± 0.05	0.34 ± 0.06	$2.25^{+0.21}_{-0.18}$
12	HIP 37504	K0 III	0.8	$4.59^{+1.52}_{-0.91}$	37.6 ± 1.5	4.39 ± 2.71	4.99 ± 3.48	0.07 ± 0.04	0.08 ± 0.06	$2.72^{+0.90}_{-0.54}$
13	HIP 38908	G0 V	1.1	$1.97^{+0.69}_{-0.42}$	49.5 ± 0.8	22.07 ± 8.03	29.09 ± 12.35	0.36 ± 0.13	0.47 ± 0.20	$1.09^{+0.38}_{-0.23}$
14	HIP 83990	K2 V	0.7	$3.92^{+1.18}_{-1.16}$	60.4 ± 1.5	3.68 ± 2.49	4.33 ± 3.72	0.06 ± 0.04	0.07 ± 0.06	$2.39^{+0.72}_{-0.71}$
15	HIP 89042	G0 V	1.1	$2.29^{+1.21}_{-0.21}$	50.6 ± 1.6	12.14 ± 4.44	14.84 ± 5.90	0.20 ± 0.07	0.24 ± 0.10	$1.27^{+0.67}_{-0.12}$
16	HIP 93506	A2 III	2.5	$3.50^{+2.31}_{-1.21}$	39.5 ± 5.7	16.62 ± 12.66	19.37 ± 16.94	0.27 ± 0.21	0.32 ± 0.28	$1.58^{+1.04}_{-0.55}$
17	HIP 114996	F1 III	1.5	$3.94^{+1.35}_{-1.77}$	29.3 ± 0.8	25.42 ± 13.03	49.78 ± 28.11	0.41 ± 0.23	0.81 ± 0.47	$2.03^{+0.70}_{-0.91}$
18	HIP 116250	G2 V	1.0	$2.79^{+2.39}_{-1.92}$	22.9 ± 1.7	33.64 ± 23.65	55.80 ± 41.51	0.55 ± 0.37	0.91 ± 0.73	$1.58^{+1.35}_{-1.09}$

Fig. 3.—Velocity changes induced by the candidate perturbers on a hypothetical objects orbiting β Pic with semimajor axis of 10^5 AU (eq. [1] and data from Table 3). *Left*: Mean velocity change for particles distributed in a shell with radius 10^5 AU. *Right*: Plot of the maximum velocity change induced by a given stellar encounter (i.e., for objects that lie closest to the perturbing star). Error bars are 1 σ (68.4% confidence level). Stars are identified by numbers given in Tables 2 and 3.

diminished because of its small mass and large relative velocity with respect to β Pic. Similarly, HIP 29958 (No. 10), with $M_* \sim 0.5\ M_\odot$ and $\Delta V_{ca} = 102.1$ km s^{-1}, does not induce on average any notably large perturbation over the orbiting comets, even at $r = 10^5$ AU. HIP 23693 (No. 6) remains then as the most significant perturber, since it combines the smallest D_{ca} in our sample, a rather small

relative velocity to β Pic (22 ± 3 km s^{-1}), and a large mass ($\sim 1.4\ M_\odot$).

4. DYNAMICAL INFLUENCE ON THE EVOLUTION OF A β PIC OORT CLOUD

The candidate stellar perturbers detected by our search cannot account for the ~ 0.005 pc close encounter simu-
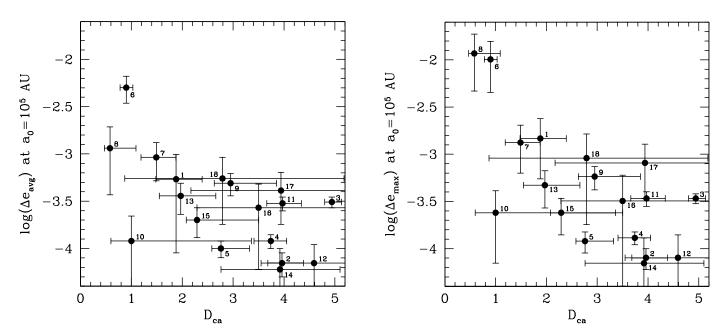

Fig. 4.—Eccentricity changes induced by the candidate perturbers on hypothetical objects orbiting β Pic with semimajor axis 10^5 AU. *Left*: Mean eccentricity change for particles distributed in a shell with radius 10^5 AU. *Right*: Plot of the maximum eccentricity change induced by a given stellar encounter (i.e., for objects that lie closest to the perturbing star). Error bars are 1 σ (68.4% confidence level). Stars are identified by numbers given in Tables 2 and 3.

lated by Kalas et al. (2000) to explain the observed dust disk morphology. However, the values for Δv and Δe at $r = 10^5$ AU may be large enough to impact the dynamical evolution of objects located beyond the detected dust disk, in a β Pic analog to the solar Oort cloud. For a circular orbit at $r = 10^5$ AU, the escape velocity for a β Pic comet, 176 m s^{-1}, is significantly greater than the orbital velocity, 124 m s^{-1}. Thus, only the cumulative effect of perturbers will dynamically modify a β Pic Oort cloud. On the other hand, the values for Δe are large enough that objects already on eccentric orbits, $e > 0.99$, could be stripped from the system after a single stellar perturbation. Moreover, objects with $r > 10^5$ AU will experience a stronger perturbation that could lead to ejection. Below we determine how the D_{ca} values for the candidate perturbers compare to the radius of a β Pic Oort cloud, and then discuss the possible evolutionary effects of the perturbations.

The maximum size of a planetesimal cloud gravitationally bound to β Pic is defined by the Roche surface of the star, a_t, set by the Galactic tidal field (Tremaine 1993):

$$a_t = 1.7 \times 10^5 \text{ AU} \left(\frac{M_*}{M_\odot}\right)^{1/3} \left(\frac{\rho}{0.15 \ M_\odot \ \text{pc}^{-3}}\right)^{-1/3} . \quad (2)$$

Holmberg & Flynn (2000) give the variance-weighted average from seven different studies of the Galactic mass density, $\rho = 0.11 \ M_\odot \ \text{pc}^{-3}$. If $M_{\beta \text{ Pic}} = 1.75 \ M_\odot$ (Crifo et al. 1997), then $a_t = 2.2 \times 10^5$ AU, or ~ 1.1 pc. Thus, at least three of the candidate perturbers (Table 2) penetrate β Pic's Roche radius.

Other perturbers, although outside the Roche radius, pass close enough to temporarily exceed the gravitational influence of the Galactic tidal field. The distance from β Pic where the gravitational forces of β Pic and the perturber on an Oort cloud comet are equal is given by (Müllari & Orlov 1996)

$$R_{eq} = d_{min}[1 - (1 + \sqrt{M_{\beta \text{ Pic}}/M_*})^{-1}] . \quad (3)$$

The last column of Table 3 gives R_{eq} for each of the candidate perturbers. In addition to the three perturbers that physically enter the Roche radius, HIP 25544 has $R_{eq} < a_t$. Thus, a total of four stars out of the 18 in Tables 1 and 2 penetrate a possible Oort cloud around β Pic.

In general, stars passing near an Oort cloud will either destroy a fraction of the cloud by sending comets into interstellar space or closer to the central star, or help build the cloud by increasing the periastron distances and hence the dynamical lifetimes of comets in the presence of planets. Stellar passages within an Oort cloud may induce comet showers, which may briefly increase dust replenishment near the star (Weissman 1996). To determine which outcome results from the stellar perturbations identified here, we must first consider whether the existence of a β Pic Oort cloud is plausible, and if so estimate its evolutionary state.

The four basic conditions for creating an Oort cloud around a star are (e.g., Fernandez 1997): (1) the formation of planetesimals in a region influenced by planets, (2) the existence of a massive planet to dynamically pump the semimajor axes of planetesimals from their formation site to large distances, (3) exogenic perturbations that decouple the planetesimals from the planets by increasing the planetesimals' periastra, and (4) sufficient time (stellar age greater than relevant timescales).

For the first condition, the existence of meter to kilometer sized planetesimals around β Pic is inferred from (1) the short lifetime of dust particles relative to β Pic's stellar age, which implies a source of replenishment, probably from the collisional erosion of larger, unseen parent bodies (Backman & Paresce 1993); and (2) variable, transient absorption features modeled as the rapid sublimation of comet-like bodies near the photosphere (Beust & Morbidelli 2000). For the second condition, indirect evidence for a massive planet at ∼1–10 AU radius is summarized in § 1. The third condition, exogenic perturbations, are expected from passing stars, molecular clouds, and the Galactic tidal field.

For the fourth condition, we compare β Pic's age, $t_{\beta \text{ Pic}}$, to the timescales required to produce an Oort cloud, as quantified by Tremaine (1993). Two of the most important timescales are the diffusion timescale, t_d, and the freezing timescale, t_f. The diffusion timescale is the time for comet apastra to diffuse out to the Roche radius of a star at constant periastra (i.e., the time for a comet's energy to reach the escape energy from repeated interactions with a planet during periastron). The freezing timescale is the time for the Galactic tide to increase comet periastra beyond the planet region, thereby freezing any further increase in the apastra. For a mature Oort cloud (i.e., well-populated and dynamically long-lived) around β Pic, we require $t_f \leq t_d < t_{\beta \text{ Pic}}$.

If $t_f > t_d$, then comet apastra will grow too quickly and achieve escape energy with one final encounter with a planet. The timescales are therefore sensitive to planet mass, M_p, and semimajor axis, a_p. If $t_{\beta \text{ Pic}} < t_d$, then the system may be in the process of forming an Oort cloud, but the comets are probably still coupled to the planetary region.

To satisfy $t_d < t_*$, Tremaine (1993) gives the following expression:

$$\frac{M_p}{M_\oplus} \geq \left(\frac{M_*}{M_\odot}\right)^{3/4} \left(\frac{t_*}{10^9 \text{ yr}}\right)^{-1/2} \left(\frac{a_p}{1 \text{ AU}}\right)^{3/4} . \quad (4)$$

For $t_f \leq t_d$, the following relation must be satisfied:

$$\frac{M_p}{M_\oplus} \leq 1.7 \left(\frac{M_*}{M_\odot}\right)^{5/7} \left(\frac{\rho}{0.15 \ M_\odot \ \text{pc}^{-3}}\right)^{2/7} \left(\frac{a_p}{1 \text{ AU}}\right)^{6/7} . \quad (5)$$

The age-independent constraint given by equation (5) is significant because it generally implies that no dynamically stable Oort cloud will form if $M_p \geq M_{\text{Saturn}}$, even for a wide range of stellar masses. For example, the Saturn-mass extrasolar planet candidates around HD 16141 and HD 46375 (Marcy, Butler, & Vogt 2000a) will not produce an extrasolar Oort cloud.

In Figure 5 we plot the regions that satisfy $t_f \leq t_d < t_{\beta \text{ Pic}}$ for a range of M_p and a_p, given $M_{\beta \text{ Pic}}/M_\odot = 1.75$, $\rho = 0.11$ $M_\odot$ pc^{-3}, and $t_{\beta \text{ Pic}} = 10^7$, 10^8, and 10^9 yr. For β Pic's estimated age of ∼10^7 yr, there is no combination of M_p and a_p that is capable of producing an Oort cloud by the present epoch that is stable from ejection. In fact, a stable Oort cloud is possible only toward the end of β Pic's lifetime, ∼10^9 yr. If we assume a combination of M_p and a_p that will eventually result in a β Pic Oort cloud (e.g., $M_p = 10 \ M_\oplus$, $a_p = 5$ AU), then at the present epoch comet apastra are only a few percent of their final values at ∼10^5 AU. The dust disk is detected in scattered light as far as ∼2×10^3 AU (Larwood & Kalas 2001), or ∼1% of the Roche radius. Depending on how future observations refine
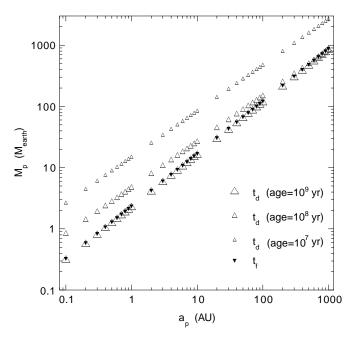
FIG. 5.—Relationship between planet parameters and Oort cloud formation timescales. Open triangles plot the constraint for the diffusion timescale, t_d, assuming three different stellar ages (eq. [4]). The t_d triangles point upward to indicate the regions of planet parameter space capable of diffusing comets to the β Pic Roche radius within the specified age ($t_d < t_*$). Below this boundary, there has been insufficient time to produce a cloud of comets with large apastra ($\sim 10^5$ AU). The timescale for freezing the semimajor axis of a comet, t_f, is shown by downward-pointing filled triangles (eq. [5]). Below the filled triangles, the Galactic tidal field decouples the comets from the planet region before ejection energy is reached ($t_f \le t_d$). Comets are ejected if the planet parameters lie above the solid triangles. A mature Oort cloud can form around β Pic only after 10^9 yr when $t_f \le t_d < t_{\beta\,\mathrm{Pic}}$.

our knowledge of a planet around β Pic, the observed dust disk may trace the early evolution of an extrasolar Oort cloud.

In summary, objects with semimajor axes near 10^5 AU might still be coupled to β Pic's planetary region. The Galactic tidal field is insufficient to decouple these objects from the planetary region before they attain escape energy. The stellar perturbations identified in our search neither eject a significant number of comets into interstellar space, nor do they cause comet showers near the star. The evolutionary role of these stellar perturbations is to build β Pic's

Oort cloud by decoupling comet periastra from the planetary region.

5. CANDIDATE PERTURBERS FOR FUTURE RADIAL VELOCITY STUDY

The most significant constraint on the completeness of this search is the lack of radial velocity information for nearly 100,000 stars in the *Hipparcos* catalog. The completion of an all-sky radial velocity survey, such as one proposed for the *GAIA* mission, has the potential to dramatically increase our knowledge of Galactic space motions.

However, given only the position, distance, and proper motion data from the *Hipparcos* catalog, it is possible to exclude the stars that would not approach β Pic for any physically meaningful value of radial velocity, and identify a sample of stars that could plausibly encounter β Pic. We adopt an iterative approach, first assuming $-120 < R_V < 120$ km s^{-1}, $\Delta R_V = 10$ km s^{-1}, to calculate D_{ca} and t_{ca} during the past 2 Myr. We select the stars with $D_{\mathrm{ca}} < 5$ pc, and repeat the procedure using $\Delta R_V = 1$ km s^{-1}, and finally $\Delta R_V = 0.1$ km s^{-1} for the stars with $D_{\mathrm{ca}} < 1$ pc. The initial positions, distances, and proper motions are fixed at the mean values given by the *Hipparcos* catalog, rather than utilizing the Monte Carlo method discussed in § 2.

The results are displayed in Tables 4 and 5. Table 4 gives the maximum number of perturbers that can be "produced" by adjusting the radial velocity in order to get the closest possible approach to β Pic. A maximum of 93 stars approach β Pic with $D_{\mathrm{ca}} < 1$ pc and $t_{\mathrm{ca}} > -1$ Myr. As expected, very close and very recent crossing events are rare, and the more the time and distance constraints are relaxed, the more events are produced. The values given in Table 4 are upper limits to the number of encounters experienced by β Pic, exceeding the expected rate of <1 pc encounters per Myr by a factor of 7.5 (§ 3).

Table 5 gives the 22 perturber candidates with $D_{\mathrm{ca}} < 0.5$ pc during the past 1 Myr. The columns list (1) name of the star, (2) distance of the closest possible approach, (3) corresponding time, (4) radial velocity that produces D_{ca}, (5) interval of radial velocities such that the distance of closest approach remains below 0.5 pc, and (6) relative velocity at the closest possible approach. Six candidate perturbers (marked with an asterisk) have $D_{\mathrm{ca}} < 0.1$ pc and are capable of perturbing the observed dust disk. Table 5 both gives a

TABLE 4

MAXIMUM NUMBER OF POSSIBLE PERTURBER CANDIDATES FROM THE *Hipparcos* CATALOG

t_{ca} (kyr)	D_{ca} (pc)									
	<0.2	<0.4	<0.6	<0.8	<1	<1.2	<1.4	<1.6	<1.8	<2
>-100	0	0	0	0	0	0	0	0	0	0
>-200	0	0	0	0	0	1	1	2	2	2
>-300	0	0	0	0	2	3	3	4	4	5
>-400	0	0	1	1	5	7	8	10	10	11
>-500	1	2	3	6	10	14	20	22	24	25
>-600	3	5	11	16	24	28	39	41	44	45
>-700	5	12	21	29	43	49	64	68	81	84
>-800	12	23	33	45	64	73	91	96	111	119
>-900	14	27	40	56	77	90	110	117	138	148
>-1000	20	36	51	70	93	111	133	141	164	174

TABLE 5
PERTURBER CANDIDATES FOR FUTURE RADIAL VELOCITY STUDIES

Hipparcos Name (1)	D_{ca} (pc) (2)	t_{ca} (kyr) (3)	R_v (km s^{-1}) (4)	$[R_v]$ ($D_{ca} < 0.5$ pc) (km s^{-1}) (5)	ΔV_{ca} (km s^{-1}) (6)
HIP 1837*	0.025	−537.0	30.6	[29.5, 31.7]	37.7
HIP 6343	0.325	−959.0	89.9	[87.8, 92.1]	78.8
HIP 6913	0.229	−560.0	88.2	[84.8, 91.9]	100.9
HIP 11324	0.127	−998.0	39.7	[38.9, 40.7]	28.9
HIP 11558	0.374	−680.0	40.8	[40.2, 41.5]	41.6
HIP 12960*	0.007	−732.0	103.7	[99.1, 108.7]	90.6
HIP 14007	0.327	−910.0	50.3	[49.1, 51.5]	34.9
HIP 14116*	0.064	−799.0	91.1	[87.1, 95.3]	74.7
HIP 22817*	0.082	−725.0	98.8	[96.3, 101.2]	97.5
HIP 26067	0.490	−283.0	110.1	[105.0, 116.1]	90.3
HIP 30260	0.480	−908.0	58.1	[56.8, 59.4]	37.6
HIP 33973*	0.077	−696.0	80.2	[77.8, 82.7]	63.3
HIP 42215	0.154	−451.0	78.7	[75.9, 81.8]	65.2
HIP 45599	0.248	−897.0	71.1	[69.4, 73.0]	58.0
HIP 51578	0.431	−924.0	88.8	[87.2, 90.5]	77.6
HIP 57949	0.237	−635.0	50.6	[49.2, 52.0]	61.3
HIP 58289	0.221	−403.0	91.0	[88.8, 93.4]	101.6
HIP 72455	0.273	−697.0	100.6	[98.2, 103.0]	101.3
HIP 78074	0.139	−792.0	59.7	[55.1, 65.0]	79.5
HIP 79789*	0.096	−871.0	80.1	[77.9, 82.3]	86.9
HIP 87435	0.110	−773.0	92.2	[88.4, 96.5]	112.9
HIP 104493	0.398	−609.0	70.1	[68.8, 71.4]	84.8

specific list of objects that require follow-up observations to determine their true radial velocities, and demonstrates the plausibility of very close stellar encounters with β Pic.

6. SUMMARY

We have tested the hypothesis that β Pic experienced a close stellar flyby by tracing the space motions of 21,497 stars 1 Myr into the past. We used the *Hipparcos* catalog for position, proper motion, and parallax data, and the Barbier-Brossat & Figon (2000) catalog for radial velocity data. The completeness of our sample is $\sim 20\%$ and is most sensitive to B–G spectral types. Our findings are:

1. In the past 1 Myr, 18 stars in our sample have had a closest approach to β Pic $D_{ca} < 5$ pc.

2. Two stars, HIP 23693 and HIP 27628, have greater than 50% probability that $D_{ca} < 1$ pc. The probability that $D_{ca} < 0.01$ pc is negligible, meaning that these encounters cannot account for the large-scale β Pic disk asymmetries modeled by Kalas et al. (2000) and Larwood & Kalas (2001).

3. The most significant dynamical perturbation on the β Pic system is due to the HIP 23693 encounter ~ 356 kyr in the past. Averaged over a hypothetical β Pic Oort cloud 0.5 pc in radius, the encounter induced a mean velocity change of $\simeq 0.3$ m s^{-1}, and eccentricity change of $\simeq 0.005$.

4. The Roche radius of β Pic set by the Galactic tidal field is ~ 1.1 pc. Four stellar perturbers penetrate the Roche radius in the past 1 Myr and could dynamically influence planetesimals bound to β Pic.

5. We summarize evidence favoring the formation of a β Pic Oort cloud. However, we find that β Pic is probably too young to have an Oort cloud that is decoupled from the planetary region. The stellar perturbations are significant in helping β Pic build its Oort cloud by pumping comet periastra away from dynamically unstable regions near planets.

6. We identify a sample of 22 stars detected by *Hipparcos* that are candidate β Pic perturbers, but require future radial velocity observations to determine their closest approach distances. Six of these stars may have $D_{ca} < 0.1$ and are potential disk perturbers.

REFERENCES

Allen, C., & Santillán, A. 1991, Rev. Mexicana Astron. Astrofis., 22, 255
———. 1993, Rev. Mexicana Astron. Astrofis., 25, 39
Backman, D. E., & Paresce, F. 1993, in Protostars and Planets III, ed. E. H. Levy & J. I. Lunine (Tucson: Univ. Arizona Press), 1253
Barbier-Brossat, M., & Figon, P. 2000, A&AS, 142, 217
Barrado y Navascues, D., Stauffer, J. R., Song, I., & Caillault, J.-P. 1999, ApJ, 520, L123
Beust, H., & Morbidelli, A. 2000, Icarus, 143, 170
Brunini, A., & Fernandez, J. A. 1996, A&A, 308, 988
Burrows, C. J., et al. 1995, BAAS, 27, 1329
Cox, A. 1999, Allen's Astrophysical Quantities (New York: AIP)
Crifo, F., Vidal-Madjar, A., Lallement, R., Ferlet, R., & Gerbaldi, M. 1997, A&A, 320, L29

de Boer, K. S., et al. 1997, A&A, 327, 577
De Medeiros, J. R., & Mayor, M. 1999, A&AS, 139, 433
European Space Agency. 1997, The Hipparcos and Tycho Catalogues (ESA SP-1200: Noordwijk: ESA)
Fernández, J. A. 1997, Icarus, 129, 106
Fernández, J. A., & Ip, W.-H. 1991, in Comets in the Post-Halley Era, ed. R. L. Newburn et al. (Dordrecht: Kluwer), 487
García-Sánchez, J., et al. 1999, AJ, 117, 1042
Goldreich, P., & Tremaine, S. 1980, ApJ, 241, 425
Greaves, J. S., et al. 1998, ApJ, 506, L133
Grenier, S., et al. 1999, A&AS, 135, 503
Heap, S. R., et al. 2000, ApJ, 539, 435
Henney, W. J., & O'Dell, C. R. 1999, AJ, 118, 2350

Holmberg, J., & Flynn, C. 2000, MNRAS, 313, 209
Johnson, D. R. H., & Soderblom, D. R. 1987, AJ, 93, 864
Kalas, P., & Jewitt, D. 1995, AJ, 110, 794
Kalas, P., Larwood, J. D., Smith, B. A., & Shultz, A. 2000, ApJ, 530, L133
Lagage, P. O., & Pantin, E. 1994, Nature, 369, 628
Lagrange, A.-M., Vidal-Madjar, A., Deleuil, M., Emerich, C., Beust, H., & Ferlet, R. 1995, A&A, 296, 499
Larwood, J. D. 1997, MNRAS, 290, 490
Larwood, J. D., & Kalas, P. 2001, MNRAS, 323, 402
Laughlin, G., & Adams, F. C. 1998, ApJ, 508, L171
Lecavelier des Etangs, A., et al. 1997, A&A, 328, 311
Liou, J.-C., & Zook, H. A. 1999, AJ, 118, 580
Malhotra, R., Duncan, M. J., & Levison, H. F. 2000, in Protostars and Planets IV, ed. V. Mannings, A. P. Boss, & S. S. Russell (Tucson: Univ. Arizona Press), in press
Marcy, G. W., Butler, R. P., & Vogt S. S. 2000a, ApJ, 536, L43
Marcy, G. W., Cochran, W. D., & Mayor, M. 2000b, in Protostars and Planets IV, ed. V. Mannings, A. P. Boss, & S. S. Russell (Tucson: Univ. Arizona Press), in press

Matthews, R. A. J. 1994, QJRAS, 35, 1
Miyamoto, M., & Nagai, R. 1975, PASJ, 27, 533
Mouillet, D., Larwood, J. D., Papaloizou, J. C. B., & Lagrange, A.-M. 1997, MNRAS, 292, 896
Müllari, A. A., & Orlov V. V. 1996, Earth Moon Planets, 72, 19
Oort, J. H. 1950, Bull. Astron. Inst. Netherlands, 11, 91
Pantin, E., Lagage, P. O., & Artymowicz, P. 1997, A&A, 327, 1123
Roques, F., Scholl, H., Sicardy, B., & Smith, B. 1994, Icarus, 108, 37
Schuster, W. J., & Allen, C. 1997, A&A, 319, 796
Smith, B., & Terrile, R. 1984, Science, 226, 1421
Tremaine, S. 1993, in ASP Conf. Ser. 35, Planets Around Pulsars, ed. J. A. Phillips, S. E. Thorsett, & S. R. Kulkarni (San Francisco: ASP), 335
Weissman, P. R. 1996, Earth Moon Planets, 72, 25
Wyatt, M. C., Dermott, S. F., Telesco, C. M., Fisher, R. S., Grogan, K., Holmes, E. K., & Pina, K. 1999, ApJ, 527, 918